Crystal structures of frozen room temperature ionic liquids, 1-ethyl-3-methylimidazolium tetrafluoroborate ($EMImBF_4$), hexafluoroniobate ($EMImNbF_6$) and hexafluorotantalate ($EMImTaF_6$), determined by low-temperature X-ray diffraction

Kazuhiko Matsumoto,[a] Rika Hagiwara,*[,a] Zoran Mazej,[b] Primož Benkič,[b] Boris Žemva[b]

[a] Graduate School of Energy Science, Kyoto University, Yoshida, Sakyo-ku, Kyoto 606-8501, Japan

[b] Department of Inorganic Chemistry and Technology, Jožef Stefan Institute, Jamova 39, SI-1000 Ljubljana, Slovenia

*E-mail: hagiwara@energy.kyoto-u.ac.jp

Key words: Room temperature ionic liquid, Ionic liquid, Room temperature molten salt, Hydrogen bonding, Structure

Abstract

The crystal structures of three salts, 1-ethyl-3-methylimidazolium tetrafluoroborate ($EMImBF_4$), hexafluoroniobate ($EMImNbF_6$) and hexafluorotantalate ($EMImTaF_6$), all of which form room-temperature ionic liquids (RTILs), have been determined by low-temperature X-ray diffraction studies of their single crystals. $EMImBF_4$ crystallizes in the monoclinic space group $P2_1/c$ with a = 8.653(5) Å, b = 9.285(18) Å, c = 13.217(7) Å, β = 121.358(15) Å, V = 906.8(19) Å^3, Z = 4 at 100 K. $EMImBF_4$ exhibits a unique structure wherein EMIm cations form one-dimensional pillars facing the imidazolium ring to the next ring linked by H(methylene)$\cdots\pi$ electron interaction. The BF_4 anion also forms one-dimensional pillars along the same direction with the nearest F$\cdots$F contact distance of 3.368(3) Å. $EMImNbF_6$ and $EMImTaF_6$ are isostructural to each other and crystallize in the orthorhombic space group $P2_12_12_1$: $EMImNbF_6$, a =9.204(4) Å, b = 9.770(15) Å, c = 12.499(13) Å, V = 1124.0(2) Å^3, Z = 4 at 200 K; $EMImTaF_6$, a = 9.216(5) Å, b = 9.763(2) Å, c = 12.502(17) Å, V = 1124.9(17) Å^3, Z = 4 at 200 K. In $EMImNbF_6$ and $EMImTaF_6$, EMIm cations also form a one-dimensional pillar structure and the hexafluorocomplex anions are located in a zigzag arrangement along the same direction with the nearest F$\cdots$F distance of 3.441(12) Å. This structure (Type-B(MF_6)) is different from the Type-A(MF_6) structure previously reported for $EMImPF_6$, $EMImAsF_6$ and $EMImSbF_6$. Hydrogen bonds in the Type-A(MF_6) ($EMImPF_6$ (333 K), $EMImAsF_6$ (326 K) and $EMImSbF_6$ (283 K)) crystal lattice are weaker than those in the Type-B(MF_6) ($EMImNbF_6$ (272 K) and $EMImTaF_6$ (275 K)) crystal lattice. This suggests that the strength of the hydrogen bond is not always a decisive and determining factor for the melting points of RTILs. The measurement of cell parameters for $EMImBF_4$ between 100 K and its melting point revealed that $EMImBF_4$ essentially preserves the same structure in this temperature range and increases its volume by only 4% due to the melting.

1. Introduction

Room-temperature ionic liquids (RTILs, also often called room-temperature molten salts) are currently widely used in various fields of electrochemistry and chemistry because of their unique properties such as nonvolatility, nonflammability and a wide liquid-state temperature range. Environmentally benign RTILs are promising solvents to replace electrolytes, reaction media and catalysts used not only in the laboratory but also on an industrial scale [1-19]. After halogenoaluminate systems, the invention of moisture-stable RTILs such as 1-ethyl-3-methylimidazolium tetrafluoroborate ($EMImBF_4$) and trifluoromethylsulfonate ($EMImCF_3SO_3$) were breakthroughs in this field [20,21] and a number of new RTILs were subsequently developed based on bulky fluoroanions such as $N(SO_2CF_3)_2^-$ [22-30]. EMIm cation-based salts have been extensively studied because they usually exhibit low melting points and high conductivities derived from relatively short but asymmetric side-chains.

Liquid structures of RTILs have been investigated using X-ray diffraction, neutron diffraction, as well as spectroscopic and computational methods [31-41]. These studies are indispensable for the understanding of physical and chemical properties of the RTILs. The solid-state structure of a salt which forms an ionic liquid is a clue to its liquid structure especially for local interactions. For EMIm salts, three halide salts, Cl^-,[42] Br^- and I^-,[43,44] were structurally characterized; EMImBr and EMImI are isostructural, whereas EMImCl exhibits a different structure. EMImF is unstable and has never been isolated under ambient conditions [45]. The structures of some halogeno-, pseudohalogeno- and oxo-anions of $EMIm^+$ have been determined including FHF^- [46], PF_6^- [22], AsF_6^-, SbF_6^- [45], $AlBr_4^-$ [44], $CoCl_4^{2-}$, $NiCl_4^{2-}$ [47], $PtCl_4^{2-}$, $PtCl_6^{2-}$, $IrCl_6^{2-}$ [48], $PdCl_4^{2-}$ [49], $AuCl_4^-$ [50], $Ag(CN)_2^-$ [51], NO_3^-, NO_2^- [20], $LaCl_6^{3-}$ [52] and $RB_{11}X_mH_n^-$ (R: alkyl, X: Br or I) [53]. In addition, solid salts based on imidazolium cations with various side-chains have also been reported including $BDMImBF_4$, $BDMImPF_6$, $BDMImSbF_6$ (BDMIm: 1-butyl-2,3-dimethylimidazolium) [54], $(EMIm)_2SO_4 \cdot H_2O$ [20], $BMImF \cdot H_2O$ (BMIm: 1-butyl-3-methylimidazolium) [55], $RB_{11}X_mH_n$ (X: Br or I) [53], $MImBiCl_4$ (MIm:1-methylimidazolium),

$DMImBiCl_4$ (1,3-dimethylimidazolium) [56], $DMImN(SO_2CF_3)_2$, $TEImN(SO_2CF_3)_2$ (1,2,3-triethylimidazolium) [57], $BMImBPh_4$ (Ph: phenyl) [58], and BMImCl [59-61]. The hydrogen bonds in these salts, which to some extent influence their properties, have been discussed previously for both solid and liquid states based on crystallographic and spectroscopic results [62]. In spite of many such previous efforts at structural studies, only a few attempts have been made thus far for determining the crystal structure of salts with melting points below room temperature [45,57]. This is because of the simple reason that these salts are liquid at room temperature, and it is technically difficult to grow and select single crystals suitable for single-crystal X-ray diffraction at low temperatures. However, the structures of such salts with low melting points need to be determined in order to elucidate the relationship between the structure and melting point, and to obtain preliminary insights into their physical and chemical properties. We have challenged the structural determination of the salts with low melting points since we first reported the crystal structure of $EMImSbF_6$ (m.p. 283 K) [45]. In this study, the crystal structures of three RTILs, $EMImBF_4$, $EMImNbF_6$ and $EMImTaF_6$, determined by low temperature X-ray diffraction will be discussed.

2. Experimental

2.1 General experimental procedure

Volatile materials were handled in vacuum lines made of stainless steel and PFA plastic, and nonvolatile materials were handled in a glovebox of dry Ar atmosphere. Anhydrous HF (Daikin Industries, Co. Ltd., purity > 99 %) was treated with K_2NiF_6 (Ozark-Mahoning) for several days prior to use in order to remove moisture. BF_3 (Nippon Sanso, purity 99.99 %), NbF_5 (Ozark-Mahoning, purity 99 %) and TaF_5 (Ozark-Mahoning, purity 99.5 %) were used as supplied. EMImCl (Sanko Chemical Industry, purity 98.5 %) was purified by recrystallization in acetonitrile solution by adding ethyl acetate. $EMIm(HF)_{2.3}F$ was synthesized by the reaction of EMImCl and aHF [63]. $EMImBF_4$, $EMImNbF_6$ and $EMImTaF_6$ were prepared by the reaction of $EMIm(HF)_{2.3}F$

and the corresponding Lewis acids (BF_3, NbF_5 and TaF_5) according to methods reported elsewhere [45].

2.2 Crystal growth and mounting

For all the compounds in this study, crystal growth was performed using the following method. Neat RTIL stored in a PFA reaction tube was cooled using liquid nitrogen and warmed to around its melting point. After this procedure was repeated several times, a crystalline substance appeared in the tube which was transferred into a cooled oil ($C_{10}F_{18}$) using a spatula cooled by liquid nitrogen. The crystal was selected from the oil and mounted on the goniometer.

2.3 X-ray diffraction analysis

X-ray diffraction data were collected using a Rigaku AFC7 diffractometer with a Mercury CCD area detector and monochromated Mo-Kα radiation at 200 K. The single crystal fixed on a glass fiber in a cooled oil ($C_{10}F_{18}$) was mounted on the goniometer head. The data obtained was processed using the CRYSTAL CLEAR program [63]. The SHELX-97 suite of programs were used for the solution and refinement of the structures [64]. All the non-hydrogen atoms were determined by the direct method and difference Fourier synthesis by introducing anisotropic displacement parameters, whereas all the hydrogen atoms were refined using appropriate riding models, with C-H distances of 0.97 Å for CH_2, 0.96 Å for CH_3 and 0.93 Å for aromatic groups. The displacement parameters of H atoms were fixed at $1.2U_{eq}$ of their parent atoms ($1.5U_{eq}$ for methyl groups). No extinction correction was performed.

3. Results and discussion

The unit cell parameters and refinement statistics for $EMImBF_4$, $EMImNbF_6$ and $EMImTaF_6$ are given in Table 1. The selected bond lengths and angles are listed in Table 2 and hydrogen bond geometries are summarized in Table 3.

3.1 Crystal Structure of $EMImBF_4$

$EMImBF_4$ crystallizes as a monoclinic lattice with a pair of ions in its asymmetric unit. The ORTEP diagram of the asymmetric unit is shown in Fig. 1. The expected intra-molecular bond lengths and angles are observed for $EMIm^+$. BF_4^- shows an almost tetrahedral geometry with B-F bond lengths in the range of 1.385–1.400 Å and F–B–F angular distortions of less than 2°. The crystal lattice consists of one-dimensional pillars along the *b*-axis (Fig. 2). EMIm cations form a pillar with the *β*-carbon of the ethyl group sticking out of the imidazolium-ring plane (C2–N1–C6–C7 torsion angle of 119.2 (4)°). The H(methylene)···π interaction (shown as dashed lines in Fig. 3) sustains the cation-cation interactions with a contact distance of 2.86 Å between H6a and the imidazolium ring centroid. Nearly the same H(methylene)···π contact (2.86 Å) was reported for $(EMIm)_2PtCl_6$ [48]. No strong interaction between the ring proton and π-electron cloud of the imidazolium ring is observed. BF_4 anions form a different pillar with a F2(i)···F2(iii) ((i): x, y, z, (iii): –x, –y, –z) distance of 3.368(3) Å and a F2···B1 distance of 4.097 (4) Å. This type of infinite ···BF_4-BF_4-BF_4···stacking is not observed in simple BF_4 salts such as alkaline metal salts ($NaBF_4$ ($CaSO_4$-type), KBF_4, $RbBF_4$ and $CsBF_4$ ($BaSO_4$-type)). This structure is also interpreted as a layered structure, wherein each layer is comprised of cation or anion pillars as seen from the upper right-hand corner to the lower left-hand corner in Fig 2 (a).

Cation-anion interactions in liquid $EMImBF_4$ were discussed by Katsyuba et al. using *ab-initio* computational and spectroscopic methods [41]. The results indicate that coulomb attractions are more dominant between the cation and anion than hydrogen bonding although some weak local

hydrogen bonds exist. Even in the solid state, hydrogen bond distances obtained for $EMImBF_4$ (Table 3) in the present study are longer than those calculated in the above report (1.936 – 2.3019 Å) by Katsyuba et al. However, two of the bond distances (2.36 Å for F1–H4 and 2.25 Å for F2–H2) can still be regarded as strong hydrogen bonds. No hydrogen bonds are observed between a fluorine atom of BF_4 and the hydrogen atom of the methylene group in $EMIm^+$ in the present study.

3.2 Crystal Structures of $EMImNbF_6$ and $EMImTaF_6$

The ORTEP diagram of the $EMImNbF_6$ asymmetric unit is shown in Fig. 4. Only the structural characteristics of $EMImNbF_6$ are described here, since $EMImTaF_6$ is isostructural to $EMImNbF_6$, with the structure being defined as Type-B(MF_6). Moreover, the cell parameters in the two cases are very close to each other due to the similarity in their ionic radii [66]. $EMImNbF_6$ crystallizes as an orthorhombic lattice containing a pair of ions in the asymmetric unit. NbF_6^- exhibits an almost octahedral geometry, with the Nb atom being located at the position of the *E* site symmetry and surrounded by six crystallographically independent fluorine atoms. Nb–F bond lengths range from 1.872 to 1.897 Å and *cis*-F–Nb–F angular distortions are less than 3°. The β-carbon of $EMIm^+$ is located above the imidazolium ring with a torsion angle of 71°. This lattice is interpreted to consist of repeating two-dimensional sheets perpendicular to the *c*-axis with an –ABCD– pattern (Fig. 5 (a)). Along the *a*-axis, a one-dimensional pillar structure is observed as in the case of $EMImBF_4$. The anion appears in a zigzag arrangement (Fig. 5 (b)) where the nearest fluorine atoms have a distance of 3.441 Å (for F5···F2). Although EMIm cations adopt a pillar-like stacking along the same direction, no short contact between the hydrogen atom and the π-electron cloud of the imidazolium ring is observed unlike in the case of $EMImBF_4$ structure (Fig 6). H···F-Nb-F···H or H···F···H bonds between the cation and the anion, shown by dashed lines in Fig. 6, contribute to the construction of this network, resulting in the formation of an alkyl-to-alkyl hydrophobic region.

As listed in Table 3, hydrogen bonds observed in $EMImNbF_6$ range from 2.40 to 2.69 Å. Unlike in the case of $EMImBF_4$, both the hydrogen atoms in the methylene group in $EMIm^+$ are involved in hydrogen bonding, especially H6b that contacts F4 with a short distance of 2.40 Å.

3.3 Structural Comparisons of $EMImBF_4$ and $EMImMF_6$ (M = P, As, Sb, Nb and Ta)

$EMImAsF_6$ and $EMImSbF_6$, whose structures were determined in our previous study, are isostructural with the $EMImPF_6$ reported previously [22,45]. This structure is defined as Type-A(MF_6). A perspective view of the $EMImAsF_6$ unit cell from the *b*-axis is shown in Fig. 7 (a), and cation-anion stacking along the *b*-axis in $EMImAsF_6$ is shown in Fig 7 (b). The unit cell parameters for Type-A(MF_6) salts are summarized in Table 4. $EMImNbF_6$ and $EMImTaF_6$, whose structures have been determined in the present study, are not isostructural with the three compounds (Type-A(MF_6)) in spite of the same octahedral geometry in all cases. Here they are called Type-B(MF_6). The ionic radii of the central atoms in the five octahedral anions increase as follows: PF_6^- (0.52 Å) < AsF_6^- (0.60 Å) < SbF_6^- (0.74 Å) < NbF_6^- (0.78 Å) ≈ TaF_6^- (0.78 Å) [66]. The structural differences are caused mostly by differences in the sizes of the anions. The larger lattice volume for $EMImSbF_6$ (1138.8(17) $Å^3$) than those for $EMImNbF_6$ (1124(2) $Å^3$) and $EMImTaF_6$ (1124.9(17) $Å^3$) in spite of the smaller size of SbF_6^- than NbF_6^- and TaF_6^- indicates that Type-A(MF_6) has a looser ion packing than Type-B(MF_6).

As is known from previous reports [22,42-44,62,67-69], the strength of the hydrogen bond in imidazolium salts depends on the basicity of the hydrogen acceptor. For example, a halide ion works as a strong acceptor, whereas large and bulky anions weakly interact with the hydrogen atom. Table 5 lists hydrogen bond geometries for Type-A(MF_6) salts ($EMImAsF_6$ and $EMImSbF_6$). The Type-A(MF_6) structure contains only a few weak hydrogen bonds (2.51 Å for the shortest H···F distances in $EMImSbF_6$ at 200K, for example) [22,45], whereas Type-B(MF_6) has a larger number of strong hydrogen bonds (2.40 Å for the shortest H···F distances in $EMImNbF_6$ at 200K, for example, as shown in Table 3). Judging from the contact distances, local hydrogen bonds in Type-

B(MF_6) are stronger than those in Type-A(MF_6) structures. Nevertheless, the Type-B(MF_6) salts exhibit lower melting points (272 K for $EMImNbF_6$ and 275 K for $EMImTaF_6$) than the Type-A(MF_6) salts (333 K for $EMImPF_6$, 326 K for $EMImAsF_6$ and 283 K for $EMImSbF_6$). $EMImBF_4$ also exhibits a low melting point of 288 K in spite of the existence of relatively strong hydrogen bonds between the cations. Different from simple inorganic ionic compounds such as NaCl with high melting points, cation-cation interactions often play an important role in imidazolium salts. In the Type-A(MF_6) structure, cations and anions alternately stack one-dimensionally along the *b*-axis to form a pillar. Strong interactions including the hydrogen bond do not exist between the cation and the anion, and no cation-cation interactions are observed. On the other hand, in the cases of the $EMImBF_4$ and Type-B(MF_6) salts, anion-anion stacking occurs resulting from the packing dominated by the hydrogen bond or molecular-like cation-cation interaction. The resulting anion-anion contact would reduce the stability of the lattice and contribute to the lowering of melting point.

3.4 Temperature dependence of the structure of EMIm salts

$EMImBF_4$ exhibits a relatively low melting point in a series of EMIm salts of the fluorocomplex anion in spite of the small sizes of BF_4^-. The cell parameters were determined at six different temperatures from 100 K to 278 K just below the melting point of $EMImBF_4$. The lattice system determined at each temperature is essentially the same as that at 100K. Figure 8 shows the temperature dependence of the molar volume of $EMImBF_4$. The lattice gradually expands with increasing temperature (expansion coefficient is 5.64×10^4 m^3 mol^{-1} K^{-1}) and an abrupt increase in the molar volume is observed at the melting point. The percentage of the molar volume change at its melting point is only 4% for $EMImBF_4$ which is much smaller than those for inorganic salts such as 25% for NaCl. This small volume change at the melting point is considered to be a peculiar property of RTILs that have bulky organic cations.

Compared to the crystallographic data in previous studies, intra-molecular bond lengths for $EMIm^+$ and BF_4^- are not sensitive to temperature variations [22,45,46-53,70]. One can easily confirm this fact by comparing the intra-molecular bond lengths for $EMIm^+$ in $EMImBF_4$ at 100 K to those in $EMImNbF_6$ and $EMImTaF_6$ at 200 K in Table 2. The contribution of the increasing temperature to the lattice expansion is due to the increase in inter-molecular distances.

Supplementary material

The supplementary material has been sent to the Cambridge Crystallographic Data Centre, 12 Union Road, Cambridge CB2 1EZ, UK, as supplementary materials No. CCDC 280603 (for $EMImBF_4$), No. 280604 (for $EMImNbF_6$) and No. 280605 (for $EMImTaF_6$) and can be obtained by contacting the CCDC.

Acknowledgements

This work was supported by a Grant-in-Aid for Scientific Research by the Japan Society for the Promotion of Science (No. 16350072), The 21st Century COE Program “Establishment of COE on Sustainable-Energy System” from the Japanese Ministry of Education, Culture, Sports, Science and Technology. One of the authors, K. Matsumoto, thanks the Japan Society for the Promotion of Science for the financial support as a research fellow.

References

[1] T. Welton, Chem. Rev. 99 (1999) 2071.

[2] K. R. Seddon, J. Chem. Technol. Biotechnol. 68 (1997) 351.

[3] P. Wasserscheid, W. Kein, Angew. Chem. Int. Ed. 39 (2000) 3772.

[4] J. Dupont, R. F. de Souza, P. A. Z. Suarez, Chem. Rev. 102 (2002) 3667.

[5] H. Olivier-Bourbigou, L. Magna, J. Mol. Catal. A 182 (2002) 419.

[6] J. D. Holbrey, K. R. Seddon, Clean Prod. Proc. 1 (1999) 223.

[7] C. M. Gordon, Appl. Catal. A 222 (2001) 101.

[8] R. Sheldon, Chem. Commun. 2001, 2399.

[9] R. Hagiwara, Y. Ito, J. Fluorine Chem. 105 (2000) 221.

[10] R. Hagiwara, Electrochemistry 70 (2002) 130.

[11] M. Ue, M. Takeda, T. Takahashi, M. Takehara, Electrochem. Solid-State Lett. 5 (2002) A119.

[12] A. Lewandowski, M. Galiński, J. Phys. Chem. Solids 65 (2004) 281.

[13] M. A. B. H. Susan, A. Noda, S. Mitsushima, M. Watanabe, Chem. Commun. 2003, 938.

[14] A. Noda, M. A. B. H. Susan, K. Kudo, S. Mitsushima, K. Hayamizu, M. Watanabe, J. Phys. Chem. B 107 (2003) 4024.

[15] R. Hagiwara, T. Nohira, K. Matsumoto, Y. Tamba, Electrochem. Solid-State Lett. 8 (2005) A231.

[16] H. Nakagawa, S. Izuchi, K. Kuwana, T. Nukuda, Y. Aihara, J. Electrochem. Soc. 150 (2003) 150, A695.

[17] H. Sakaebe, H. Matsumoto, Electrochem. Commun. 5 (2003) 594.

[18] N. Koura, K. Etoh, Y. Idemoto, F. Matsumoto, Chem. Lett. 2001, 1320.

[19] N. Papageorgiou, Y. Athanassov, M. Armand, P. Bonhôte, H. Pettersson A. Azam, M. Grätzel, J. Electrochem. Soc. 143 (1996) 3099.

[20] J. S. Wilkes, M. J. Zaworotko, J. Chem. Soc., Chem. Commun. 1992, 965.

[21] E. I. Cooper, J. M. O'Sullivan, Proc. of 8th Int. Sym. Molten Salts, 1992, 386.

[22] J. Fuller, R. T. Carlin, H. C. De Long, D. Haworth, J. Chem. Soc., Chem. Commun. 1994, 299.

[23] S. Shirakami, Chem. Lett. 2001, 262.

[24] C. E. Song, W. H. Shim, E. J. Roh, J. H. Choi, J. Chem. Soc., Chem. Commun. 2000, 1695.

[25] T. Itoh, E. Akasaki, K. Kudo, S. Shirakami, Chem. Lett., 2001, 262.

[26] S. Forsyth, J. Golding, D. R. MacFarlane, M. Forsyth, Electrochim. Acta 46 (2001) 1753.

[27] D. R. MacFarlane, P. Meakin, J. Sun, N. Amini, M. Forsyth, J. Phys. Chem. B 103 (1999) 4164.

[28] R. P. Singh, S. Manandhar, J. M. Shreeve, Tetrahedron Lett. 43 (2002) 9497.

[29] C. M. Jin, J. M. Shreeve, Inorg. Chem. 43 (2004) 7532.

[30] P. Bonhôte, A. -P. Dias, M. Armand, N. Papageorgiou, K. Kalyanasundaram, M. Grätzel, Inorg. Chem. 35 (1996) 1168.

[31] C. Hardacre, J. D. Holbrey, S. E. J. McMath, D. T. Bowron, A. K. Soper, J. Chem. Phys. 118 (2003) 273.

[32] S. Takahashi, K. Suzuya, S. Kohara, N. Koura, L. A. Curtiss, M. -L. Saboungi, Z. Phys. Chem. (Munich) 209 (1999) 209.

[33] E. A. Turner, C. Cory, R. D. Singer, J. Phys. Chem. A 107 (2003) 2277.

[34] C. G. Hanke, N. A. Atamas, R. M. Lynden-Bell, Green Chem. 4 (2002) 107.

[35] C. G. Hanke, S. L. Price, R. M. Lynden-Bell, Mol. Phys. 99 (2001) 801.

[36] J. K. Shah, J. F. Brennecke, E. J. Maginn, Green Chem. 4 (2002) 112..

[37] J. de Andrade, E. S. Böes, H. Stassen, J. Phys. Chem. B 106 (2002) 13344.

[38] J. de Andrade, E. S. Böes, H. Stassen, J. Phys. Chem. B 106 (2002) 3546.

[39] R. Hagiwara, K. Matsumoto, T. Tsuda, Y. Ito, S. Kohara, K. Suzuya, H. Matsumoto, Y. Miyazaki, J. Non-Cryst. Solids 312-314 (2002) 414.

[40] K. Matsumoto, R. Hagiwara, Y. Ito, S. Kohara, K. Suzuya, Nucl. Instrum. Meth. B. 199 (2003) 29.

[41] S. A. Katsyuba, P. J. Dyson, E. E. Vandyukova, A. V. Chernova, A. Vidiš, Helv. Chim. Acta 87 (2004) 2556

[42] C. J. Dymek Jr., D. A. Grossie, A. V. Fratini, W. W. Adams, J. Mol. Struc. 213 (1989) 25.

[43] A. K. Abudul-Sada, A. M. Greenway, P. B. Hitchcock, T. J. Mohammed, K. R. Seddon, J. A. Zora, J. Chem. Soc., Chem. Commun. 1986, 1753.

[44] A. Elaiwai, P. B. Hitchcock, K. R. Seddon, N. Srinivasan, Y. Tan, T. Welton, J. A. Zora, J. Chem. Soc., Dalton Trans. 1995, 3467.

[45] K. Matsumoto, R. Hagiwara, R. Yoshida, Y. Ito, Z. Mazej, P. Benkič, B. Žemva, O. Tamada, H. Yoshino, S. Matsubara, Dalton Trans., 2004, 144.

[46] K. Matsumoto, T. Tsuda, R. Hagiwara, Y. Ito, O. Tamada, Solid State Sci. 4 (2002) 23.

[47] P. B. Hitchcock, K. R. Seddon, T. Welton, J. Chem. Soc., Dalton Trans. 1993, 2639.

[48] M. Hasan, I. V. Kozhevnikov, M. R. H. Siddiqui, C. Femoni, A. Steiner, N. Winterton, Inorg. Chem. 40 (2001) 795.

[49] M. F. Ortwerth, M. J. Wyzlic, R. G. Baughman, Acta Cryst. C54 (1998) 1594

[50] M. Hasan, I. V. Kozhevnikov, M. R. H. Siddiqui, A. Steiner, N. Winterton, Inorg. Chem. 38 (1999) 5637.

[51] Y. Yoshida, K. Muroi, A. Otsuka, G. Saito, M. Takahashi, T. Yoko, Inorg. Chem. 43 (2004) 43, 1458.

[52] K. Matsumoto, T. Tsuda, T. Nohira, R. Hagiwara, Y. Ito, O. Tamada, Acta Cryst. C58 (2002) m186.

[53] A. S. Larsen, J. D. Holbrey, F. S. Tham, C. A. Reed, J. Am. Chem. Soc. 122 (2000) 7264.

[54] P. Kölle, R. Dronskowski, Eur. J. Inorg. Chem., 2004, 2313.

[55] R. P. Swatloski, J. D. Holbrey, R. D. Rogers, Green Chem. 5 (2003) 361.

[56] D. J. Williams, W. T. Pennington, D. VanDerveer, J. T. Anderton, K. M. White, J. Chem. Cryst. 33 (2003) 465.

[57] J. D. Holbrey, W. M. Reichert, R. D. Rogers, Dalton Trans., 2004, 2267.

[58] J. Dupont, P. A. Z. Suarez, R. E. De Souza, R. A. Burrow, J. -P. Kintzinger, Chem. Eur. J. 6 (2000) 2377.

[59] S. Hayashi, R. Ozawa, H. Hamaguchi, Chem. Lett. 32 (2003) 498.

[60] S. Saha, S. Hayashi, A. Kobayashi, H. Hamaguchi, Chem. Lett. 32 (2003) 740.

[61] J. D. Holbrey, W. M. Reichert, M. Nieuwenhuyzen, S. Johnston, K. R. Seddon, R. D. Roger, Chem. Commun. 2003, 1636.

[62] A. G. Avent, P. A. Chaloner, M. P. Day, K. R. Seddon, T. Welton, J. Chem. Soc., Dalton Trans. 1994, 3405.

[63] R. Hagiwara, K. Matsumoto, Y. Nakamori, T. Tsuda, Y. Ito, H. Matsumoto, K. Momota, J. Electrochem. Soc. 150 (2003) D195.

[64] CRYSTALCLEAR, Rigaku Corporation, Woodlands, TX, 1999.

[65] G. M. Sheldrick, SHELX-97, University of Göttingen, Germany, 1997.

[66] R. D. Shannon, Acta Cryst. A32 (1976) 751.

[67] S. Tait, R. A. Osteryoung, Inorg. Chem., 23 (1984) 4352.

[68] J. L. E. Campbell, K. E. Johnson, J. R. Torkelson, Inorg. Chem. 33 (1994) 3340.

[69] K. M. Dieter, C. L. Dymek, N. E. Helmer, J. W. Rovang, J. S. Wilkes, J. Am. Chem. Soc. 110 (1988) 2722.

[70] M. J. R. Clark, H. Lynton, Can. J. Chem. 47 (1969) 2579.

Table 1 Crystal data and refinement results for $EMImBF_4$, $EMImNbF_6$ (Type-B(MF_6)) and $EMImTaF_6$ (Type-B(MF_6))

	$EMImBF_4$	$EMImNbF_6$	$EMImTaF_6$
Empirical formula	$H_{11}C_6N_2F_4B_1$	$H_{11}C_6N_2F_6Nb_1$	$H_{11}C_6N_2F_6Ta_1$
Formula weight	197.98	318.08	406.12
Crystal system	Monoclinic	Orthorhombic	Orthorhombic
Space group	$P2_1/c$	$P2_12_12_1$	$P2_12_12_1$
a / Å	8.653(5)	9.204(4)	9.216(5)
b / Å	9.285(18)	9.770(15)	9.763(2)
c / Å	13.217(7)	12.499(13)	12.502(17)
β/ °	121.358(15)	-	-
V / Å	906.8(19)	1124(2)	1124.9(17)
Z	4	4	4
d_c / g cm^{-3}	1.450	1.880	2.398
μ / mm^{-1}	0.145	1.122	9.823
T / K	100	200	200
T_m / K [a]	288	272	275
R_1 ($I>2\sigma(I)$) [b]	0.0577	0.0549	0.0417
wR_2 ($I>2\sigma(I)$) [c]	0.1706	0.1385	0.0953

[a] T_m: Melting point (see ref. 45) [b] $R_1 = \Sigma||F_o|-|F_c||/\Sigma|F_o|$.

[c] $wR_2 = [\Sigma w[|F_o|^2-|F_c|^2]^2/\Sigma w|F_o|^2]^{1/2}$

Table 2 Selected bond lengths (Å) and angles (deg) for $EMImBF_4$ (at 100 K), $EMImNbF_6$ and $EMImTaF_6$ (at 200 K)

	$EMImBF_4$	$EMImNbF_6$	$EMImTaF_6$
$EMIm^+$:			
N1–C2	1.323(4)	1.331(11)	1.289(12)
C2–N3	1.337(4)	1.319(10)	1.319(13)
N3–C4	1.383(4)	1.384(12)	1.375(12)
C4–C5	1.358(5)	1.341(11)	1.347(14)
C5–N1	1.391(4)	1.382(11)	1.369(12)
N1–C6	1.472(4)	1.460(10)	1.477(11)
C6–C7	1.508(5)	1.523(14)	1.495(15)
N3–C8	1.456(4)	1.474(11)	1.480(11)
N1–C2–N3	108.8(3)	108.7(7)	109.0(8)
C2–N3–C4	108.3(3)	109.6(7)	108.9(9)
N3–C4–C5	107.4(3)	105.7(8)	105.7(9)
C4–C5–N1	106.4(3)	108.5(10)	107.1(10)
C5–N1–C2	109.0(3)	107.5(7)	109.2(9)
C2–N1–C6	124.6(3)	126.4(7)	125.9(9)
C5–N1–C6	126.4(3)	126.0(8)	124.6(9)
N1–C6–C7	112.0(3)	112.6(8)	112.0(10)
C2–N3–C8	125.7(3)	124.2(8)	125.3(8)
C4–N3–C8	125.9(3)	126.3(7)	125.8(9)
C2–N1–C6–C7	119.2(4)	104.7(11)	104.9(13)
MF_m^- (M=B, Nb, Ta):			
M–F1	1.385(4)	1.881(6)	1.886(6)
M–F2	1.398(4)	1.872(6)	1.881(6)
M–F3	1.385(4)	1.883(6)	1.866(6)
M–F4	1.400(4)	1.897(6)	1.896(6)
M–F5	-	1.872(6)	1.858(6)
M–F6	-	1.875(6)	1.878(7)
F1–M–F2	109.6(3)	89.8(3)	90.5(3)
F1–M–F3	110.8(3)	177.4(3)	177.3(3)
F1–M–F4	109.5(3)	88.2(3)	87.5(3)
F1–M–F5	-	91.5(3)	91.4(4)
F1–M–F6	-	89.1(3)	88.8(3)
F2–M–F3	109.5(3)	92.5(3)	92.2(3)
F2–M–F4	108.5(3)	177.7(3)	178.0(3)
F2–M–F5	-	90.3(3)	90.8(3)
F2–M–F6	-	92.2(3)	91.6(3)
F3–M–F4	108.9(3)	89.5(3)	89.8(3)
F3–M–F5	-	89.7(3)	89.1(3)
F3–M–F6	-	89.6(3)	90.6(4)
F4–M–F5	-	88.6(3)	88.8(3)
F4–M–F6	-	88.9(3)	88.7(3)
F5–M–F6	-	177.5(3)	177.5(3)

Table 3 Hydrogen bonding geometries for $EMImBF_4$, $EMImNbF_6$ and $EMImTaF_6$ (Å, deg)

D–H··*A*	*D*–H	H··*A*	*D*··*A*	*D*–H··*A*
$EMImBF_4$				
C(2)–H(2)···F(2)[a]	0.93	2.59	3.120(4)	116.6
C(2)–H(2)···F(2)[a]	0.93	2.25	3.113(4)	154.6
C(2)–H(2)···F(4)	0.93	2.66	3.080(3)	108.2
C(4)–H(4)···F(1)	0.93	2.36	3.204(4)	149.7
C(5)–H(5)···F(3)	0.93	2.49	3.409(4)	166.5
C(5)–H(5)···F(4)	0.93	2.62	3.289(4)	129.4
C(7)–H(7a)···F(2)	0.96	2.60	3.510(4)	157.4
C(7)–H(7b)···F(1)	0.96	2.68	3.446(4)	136.9
C(8)–H(8a)···F(2)	0.96	2.57	3.351(4)	138.6
C(8)–H(8c)···F(4)	0.96	2.45	3.299(4)	147.8
$EMImNbF_6$				
C(2)–H(2)···F(3)	0.93	2.63	3.331(10)	132.2
C(4)–H(4)···F(3)	0.93	2.41	3.174(11)	139.7
C(5)–H(5)···F(2)	0.93	2.69	3.172(13)	113.1
C(5)–H(5)···F(5)	0.93	2.49	3.328(11)	150.2
C(6)–H(6a)···F(3)	0.97	2.56	3.286(12)	131.7
C(6)–H(6b)···F(4)	0.97	2.40	3.319(11)	158.1
C(7)–H(7a)···F(6)	0.96	2.57	3.443(12)	151.3
C(8)–H(8a)···F(2)	0.96	2.51	3.318(13)	142.3
C(8)–H(8b)···F(4)	0.96	2.53	3.258(12)	132.8
C(8)–H(8c)···F(1)	0.96	2.60	3.166(13)	118.0
$EMImTaF_6$				
C(2)–H(2)···F(3)	0.93	2.63	3.339(12)	133.0
C(4)–H(4)···F(3)	0.93	2.46	3.212(12)	138.6
C(5)–H(5)···F(2)	0.93	2.66	3.157(13)	113.8
C(5)–H(5)···F(5)	0.93	2.48	3.324(13)	151.7
C(6)–H(6a)···F(3)	0.97	2.55	3.278(14)	132.2
C(6)–H(6b)···F(4)	0.97	2.42	3.340(13)	158.2
C(7)–H(7a)···F(6)	0.96	2.62	3.485(14)	150.8
C(8)–H(8a)···F(2)	0.96	2.60	3.318(13)	132.1
C(8)–H(8b)···F(4)	0.96	2.67	3.265(12)	120.5

[a] The two F atoms labeled F(2) belong to different BF_4 anions.

Table 4 Unit cell parameters for EMIm salts with the Type-A(MF_6) structure; $EMImPF_6$, $EMImAsF_6$ and $EMImSbF_6$

	$EMImPF_6$ [a]	$EMImAsF_6$ [b]	$EMImSbF_6$ [b]
Empirical formula	$H_{11}C_6N_2F_6P_1$	$H_{11}C_6N_2F_6As_1$	$H_{11}C_6N_2F_6Sb_1$
Formula weight	255.24	300.09	346.92
Crystal system	Monoclinic	Monoclinic	Monoclinic
Space group	$P2_1/c$	$P2_1/c$	$P2_1/c$
a / Å	8.757(2)	8.871(10)	8.942(8)
b / Å	9.343(2)	9.424(2)	9.390(8)
c / Å	13.701(3)	13.786(2)	13.849(12)
β/ °	103.05(3)	102.985(14)	101.680(12)
V / Å	1092.02	1123.04(3)	1138.8(17)
Z	4	4	4
d_c / g cm^{-3}	1.558	1.775	2.024
T / K	283-303	298	200
T_m / K [c]	333	326	283

[a] Ref. 22. [b] Ref. 45 [c] T_m: Melting point (see Ref. 45)

Table 5 Hydrogen bond geometries for $EMImAsF_6$ at 298 K and $EMImSbF_6$ at 200 K (Å, deg) (from Ref. 45)

D–H··*A*	*D*–H	H··*A*	*D*··*A*	*D*–H··*A*
$EMImAsF_6$				
C(2)–H(2)…F(1)	0.93	2.59	3.254(4)	129
C(2)–H(2)…F(5)	0.93	2.67	3.137(4)	112
C(8)–H(8b)…F(1)	0.96	2.54	3.396(3)	148
C(8)–H(8c)…F(3)	0.96	2.62	3.300(3)	128
C(8)–H(8a)…F(6)	0.96	2.69	3.221(4)	115
$EMImSbF_6$				
C(2)–H(2)…F(1)	0.93	2.51	3.228(5)	134
C(2)–H(2)…F(5)	0.93	2.68	3.108(7)	109
C(8)–H(8b)…F(1)	0.96	2.55	3.345(6)	140
C(8)–H(8c)…F(3)	0.96	2.71	3.304(6)	121
C(8)–H(8a)…F(6)	0.96	2.59	3.129(7)	116

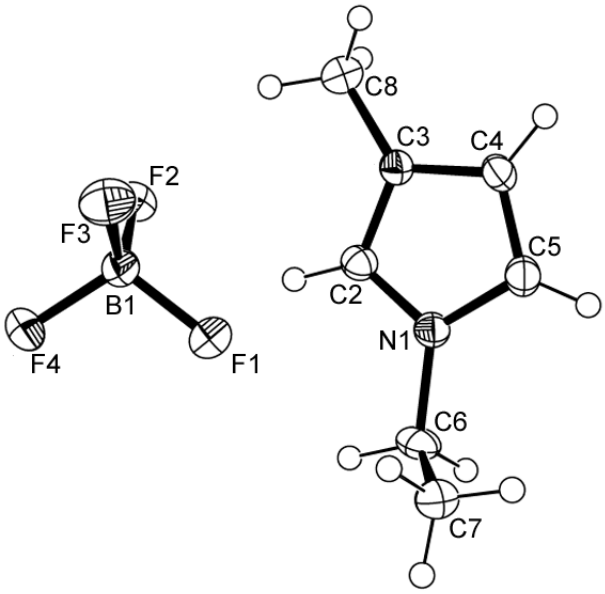

Fig. 1 ORTEP diagram of $EMIm^+$ and BF_4^- in the $EMImBF_4$ structure with an atom numbering scheme. Displacement ellipsoids are shown at a 50 % probability level and hydrogen atoms are drawn as small circles of arbitrary radii.

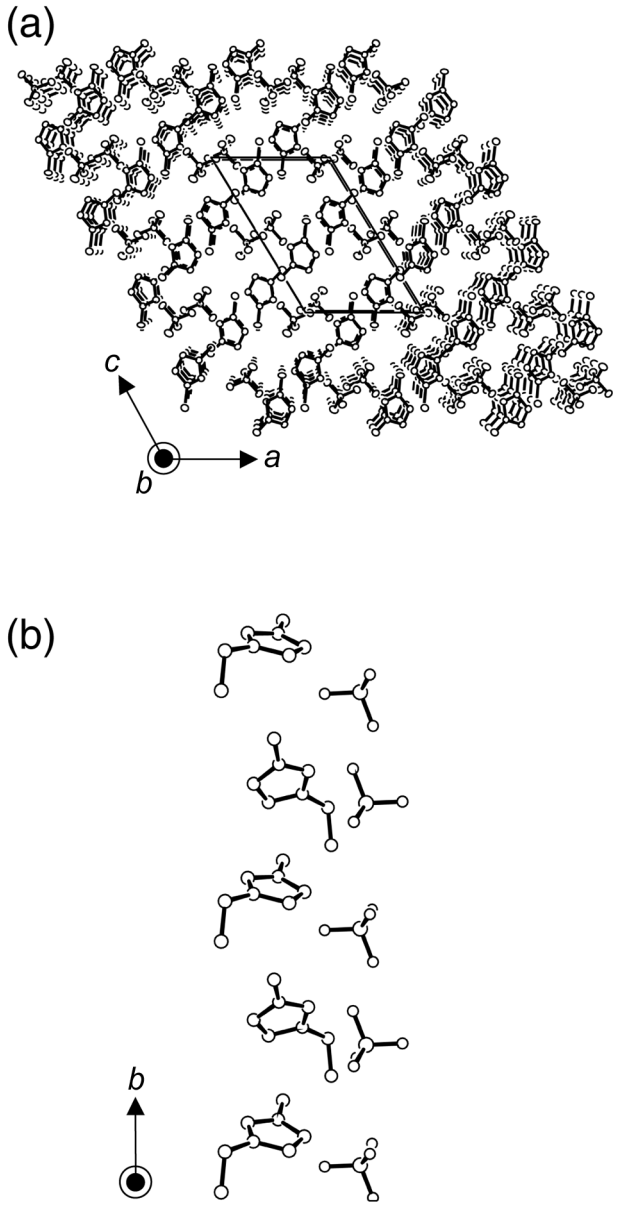

Fig. 2 Molecular packing in the $EMImBF_4$ structure: (a) Perspective view from the *b*-axis and (b) cation-cation and anion-anion stacking along the *b*-axis.

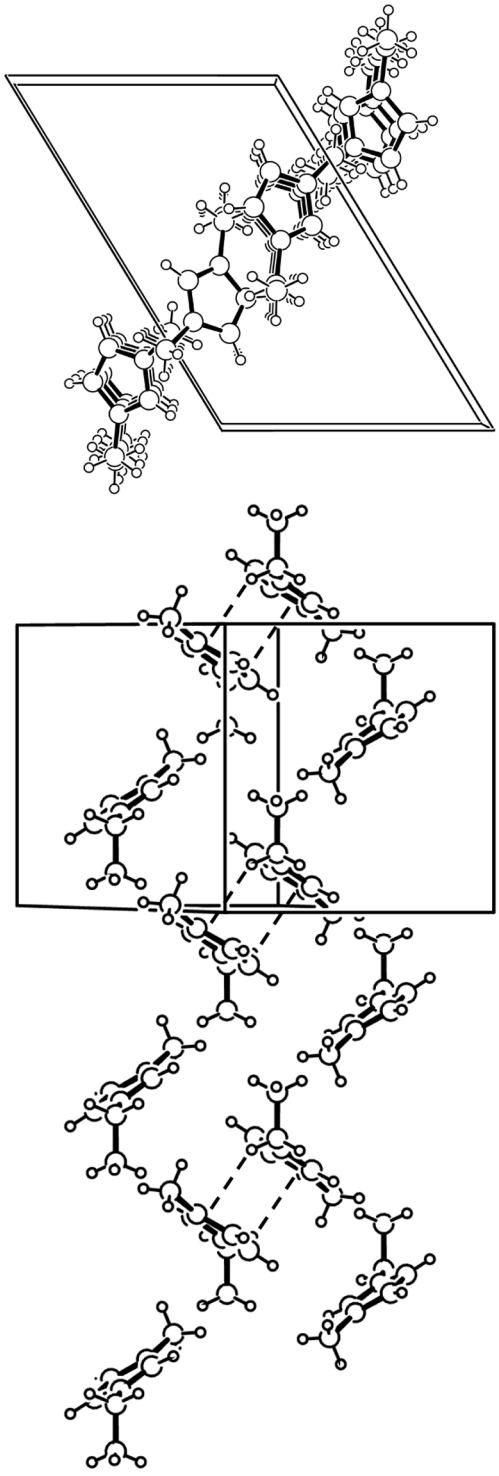

Fig. 3 Cation-cation interaction along the *b*-axis in the $EMImBF_4$ structure. The bottom drawing is the view perpendicular to the top one. The anions are omitted for clarity.

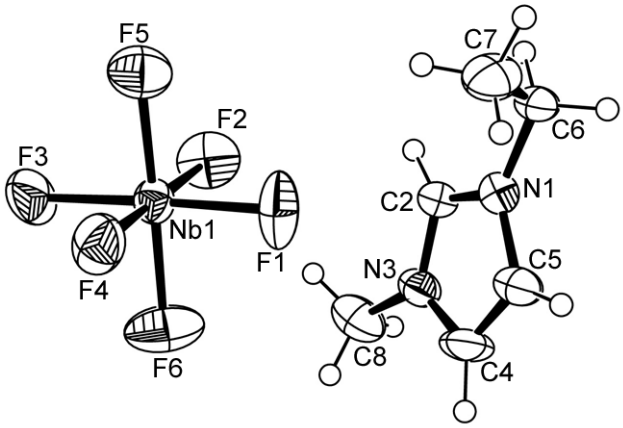

Fig. 4 ORTEP diagram of $EMIm^+$ and NbF_6^- in the $EMImNbF_6$ structure with an atom numbering scheme. Displacement ellipsoids are shown at 50 % probability level and hydrogen atoms are drawn as small circles of arbitrary radii.

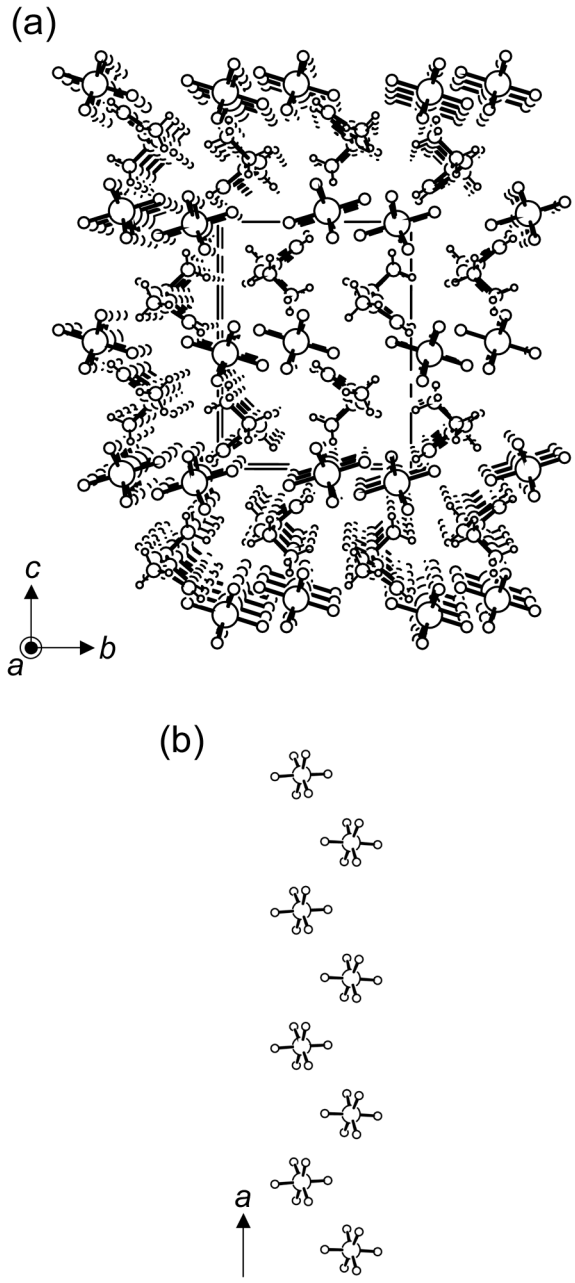

Fig. 5 Molecular packing in the $EMImNbF_6$ structure: (a) Perspective view from the *a*-axis and (b) zig-zag arrangement of the anion along the *a*-axis.

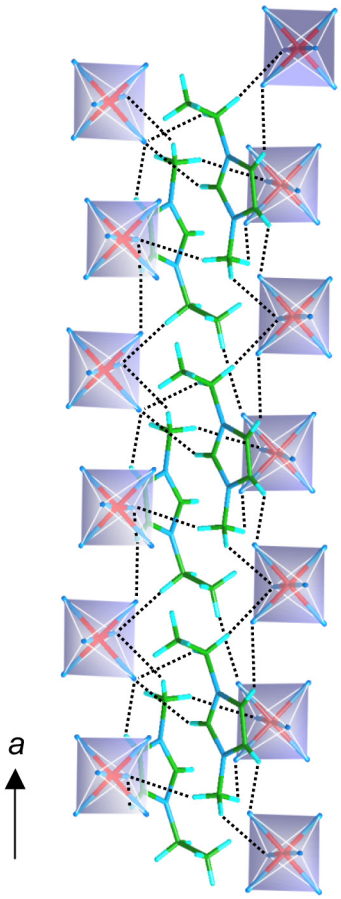

Fig. 6 Ion-ion interactions in the $EMImNbF_6$ structure. The dashed line shows hydrogen bonding between a hydrogen atom in $EMIm^+$ and a fluorine atom of NbF_6^-.

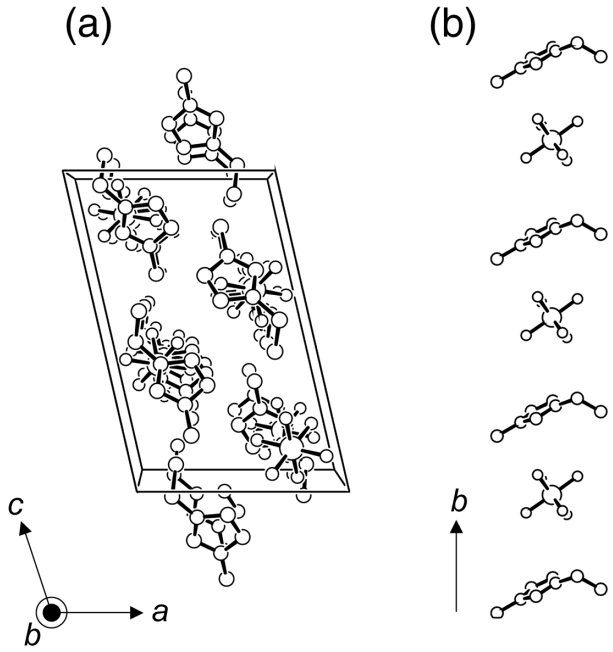

Fig. 7 Molecular packing in the $EMImAsF_6$ structure: (a) Perspective view from the *b*-axis and (b) caion-anion alternative stacking along the *b*-axis.

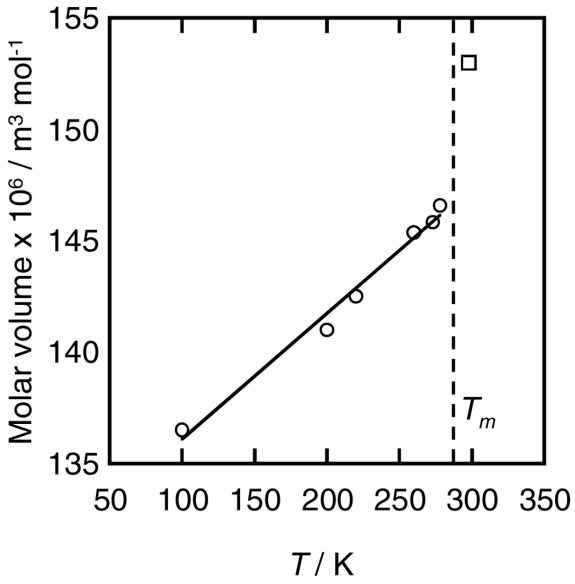

Fig. 8 Temperature dependence of the molar volume of $EMImBF_4$. Open circles represent the values in the solid state and the open squares in the liquid state.

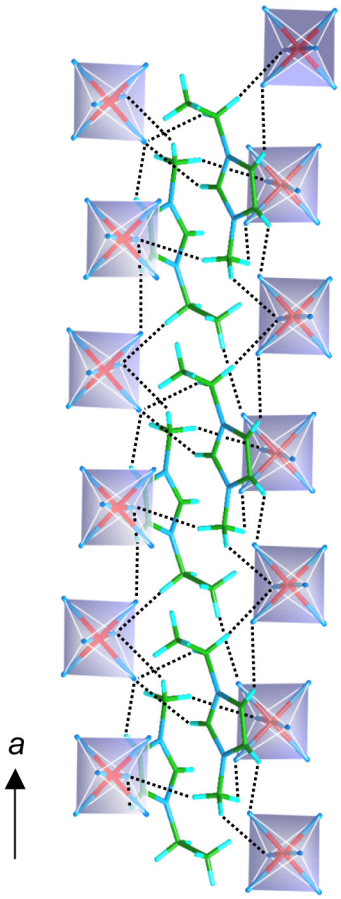

Graphical abstract